

Harmonics Elimination in PWM Inverters Using Neural Network

P.P. Mohanlal and S. Dasgupta

Control and Guidance Design Group,
Vikram Sarabhai Space Centre,
Thiruvananthapuram — 695 022

Abstract:

Programmed PWM schemes require many waveforms to be stored in memory for varying values of output fundamental magnitudes. It is only useful for harmonic reduction when the drive is operating in the steady state and not for operation in the transient state. The applicability of Neural Network for harmonic reduction in PWM inverters is established to handle the continuous variation of output fundamental amplitude. A method suggested to incorporate the random phase modulation of the switching angles with the Neural scheme to smear the concentrated energy at the switching frequency. The limitation of the random modulation, specially at low control ratios and the usefulness of the Neural scheme are brought out.

INTRODUCTION

The purpose of PWM (pulse width modulation) in inverters is to change the ratio of the fundamental of the ac voltage to the dc voltage. Some of the modulation schemes employed are endpulse modulation, centrepulse modulation, sinusoidal PWM, stair case PWM etc. The switched waveforms in these modulation schemes contain low order harmonics which are often unacceptable. All these modulation schemes maintain symmetry in the switched waveform due to which the even harmonics will be absent. A typical switched waveform of single phase is shown in Fig. 1 in which symmetry is maintained. By reversing the phase potentials a number of times during each half cycle, the spectra of harmonics can be changed in such a way that some low order harmonics troublesome to the load are cancelled where as some higher order harmonics which are less harmful increase in magnitude. The notches are placed symmetrically about the centre of each half cycle to maintain symmetry.

A waveform with the angles of reversal equal to $\alpha_1, \alpha_2, \alpha_3, \dots, \alpha_p$ has the following rms values of the n th harmonic voltage

$$U(n) = (0.45 / n) u_d \{ 2(\cos n\alpha_1 - \cos n\alpha_2 + \cos n\alpha_3 - \dots) - 1 \} \dots \dots (1)$$

where $U(n)$: amplitude of n th harmonic
 u_d : Input DC voltage
 n : harmonic number

γ (control ratio) : (actual fundamental / fundamental of unmodulated wave)

For example, control of the fundamental and cancellation of the 5th and 7th harmonics will result in the following system of nonlinear equations[4].

$$2(\cos \alpha_1 - \cos \alpha_2 + \cos \alpha_3) - 1 = \gamma \dots \dots \dots (2)$$

$$2(\cos 5\alpha_1 - \cos 5\alpha_2 + \cos 5\alpha_3) - 1 = 0 \dots \dots \dots (3)$$

$$2(\cos 7\alpha_1 - \cos 7\alpha_2 + \cos 7\alpha_3) - 1 = 0 \dots \dots \dots (4)$$

Each of the reversal corresponds to one degree of freedom, making it possible either to cancel a harmonic or to control the fundamental voltage. In programmed PWM, the switching angles from Equations. (2) - (4) are precomputed numerically for different discrete values of γ and stored for use.

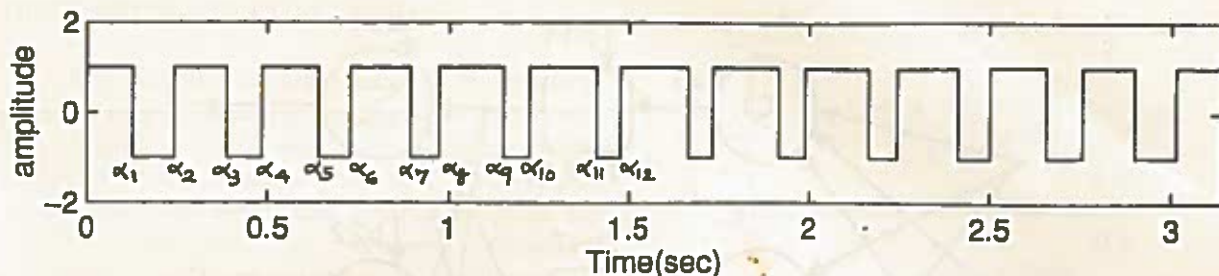


Fig. 1 , PWM switched waveform for half period ($\gamma = 0.37$)

This requires many waveforms to be stored in addition to other limitations.

If we choose an even number (p) of switching angles, there will be $(p-1)$ number of odd harmonics below the switching frequency $f_s = (2p+1)f$, where f is the fundamental frequency. Now we can have p number of equations of the type (2) - (4) with p unknown switching angles ($\alpha_1, \alpha_2, \alpha_3, \dots, \alpha_p$) for a given value of control ratio. Thus for a given control ratio, p switching angles can be solved from these equations to null all the $(p-1)$ odd harmonics below the switching frequency. This will result in no harmonics energy below switching frequency.

DESIGN PARAMETERS AND TRAINING DATA FOR NEURAL NETWORK.

In this study, $p = 12$, $f = 1$ rad/sec, $f_s = 25$ rad/sec. There are 11 odd harmonics below f_s to be nulled. 12 equations of the type (2) - (4) are formed and solved using gradient method for $\gamma = 0.02, 0.04, 0.06, \dots, 0.74$ to get 12 switching angles for each value of γ . This data set is used to train the Neural Network. Sample data in degrees, for $\gamma = 0.02$ to 0.20 are tabulated in Table.1.

TRAINING OF NEURAL NETWORK

It is well known that suitably selected feedforward neural network can approximate any arbitrary nonlinear static mapping with desired accuracy. When the training data spans the input space reasonably, the network can interpolate the function quite well for untrained inputs. Multilayer feedforward and Radial

basis networks are commonly employed for the above purpose.

Radial basis networks require less training time and interpolate well if the training data spans the input space uniformly. For this application, the radial basis network was found to be more suitable from the point of view of training time, interpolation accuracy and number of neurons. The basic form of the radial basis neural network with r -inputs, m -outputs and q -radial basis neurons is shown in Fig. 2. Orthogonal least squares training algorithm [1] is used for the training of the network. The spread constant is chosen as 0.08. The sum squared error could be reduced to less than $10e-10$ with just 29 neurons in the radial basis layer.

Training inputs are the different γ values from 0.02 to 0.74. For each scalar input, there are 12 outputs ($\alpha_1, \alpha_2, \dots, \alpha_{12}$) which means that 12 neurons in the output layer. The training data generated is used to train the network. To ascertain the interpolation accuracy, the test data set is generated as follows. For $\gamma = 0.01, 0.03, \dots, 0.73$, the corresponding firing angle vectors are again computed by gradient method and used to test the network for interpolation accuracy.

This sample data for $\gamma = 0.01$ to 0.19 are tabulated in Table 2. Fig. 3a, 3b and 3c give the training error and interpolation accuracy respectively for training inputs and test inputs. The interpolation error is less than $5e-5$.

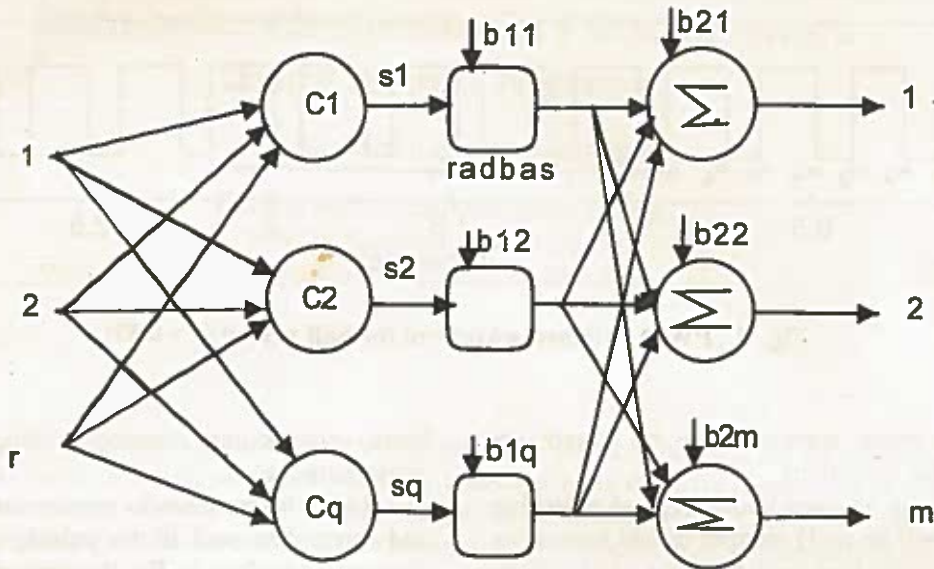


Fig. 2 , Radial Basis Neural Network.

Where,

C_1, C_2, \dots, C_q are radial centres of dimension R^1

s_1, s_2, \dots, s_q are the Euclidean distances between input and radial centres. (i.e. $s_1 = \text{input} - C_1$, etc.).

$\text{radbas}(s_1, b_{11}) = \exp(-(b_{11} * s_1)^2)$

$b_{11}, b_{12}, \dots, b_{1q} = (0.8326)/(\text{spread constant})$

$b_{21}, b_{22}, \dots, b_{2m}$: bias inputs

SIMULATION AND ANALYSIS OF SWITCHED PWM WAVEFORM

Three control ratios ($\gamma = 0.01, 0.37, 0.73$) are chosen to test the Neural Network based PWM switching scheme. It is to be noted that the network was not trained for these inputs. Fig 5a, 5b and 5c give the spectral output of the switched waveform. The harmonics below switching frequency are almost invisible. The linearity of the output amplitude with respect to the control ratios is given in Fig 4.

SIMULATION OF RANDOM MODULATION OF SWITCHING ANGLES AND SMEARING OF SWITCHING TONE ENERGY

In [2, 3], random modulation of the carrier of the sine PWM was used to reduce the acoustic noise in

PWM drives. The idea is that using random modulation, the energy concentrated at switching frequency can be made to spread over a desired frequency range. This is achieved with the average switching frequency the same as the unmodulated case, unlike other schemes where switching frequency is very high.

In the present Neural Net PWM, to achieve random modulation, uniformly distributed, amplitude limited (-7 to 7), zero mean random sequence is generated and added to each phase angle output of the Neural Network. The resulting PWM waveform will have average switching frequency same as the unmodulated case. The spectral analysis of the output waveform with random modulation is given in Fig 6a, 6b and 6c for the three cases for which the unmodulated spectra are in Fig 5a, 5b and 5c respectively.

Here, for $\gamma = 0.73$, the random modulation is found to be useful. Where as for $\gamma = 0.01$, the random modulation makes the output completely useless. For $\gamma = 0.37$, the effect is moderate. This means that random modulation is useful only at higher control ratios in PWM drives.

DISCUSSION AND CONCLUSIONS

The Neural Network based PWM switching scheme has good linearity and harmonic rejection. It has the ability of real time and continuous output amplitude control. Random phase modulation can be incorporated with the Neural scheme to spread the energy concentrated at switching frequency even though random modulation is useful only at high control ratios.

The switching frequency can be increased by increasing the number of phase angle reversal points. For example, with $p = 24$, f_s nearly doubles (49 rad/sec). Since all the harmonics below switching frequency can be nulled, it is desirable to choose an appropriate value of p such that the resulting switching frequency does not harm the load. This is a better scheme than the random modulation method since the later is not useful at low control ratios. However, the option of random modulation can be retained with Neural Net based PWM.

The Neural Net based PWM is better than programmed PWM due to its capability to handle continuous amplitude control. It is also better than the random modulation scheme since the later is not useful at low control ratios. The hardware implementation aspects need to be explored.

REFERENCES

1. S.Chen, C.F.N. Cowan & P.M. Grant, Orthogonal Least Squares learning algorithm, IEEE Trans on Neural Networks, vol 2, no.2, pp302-309, March 1991.
2. T.G.Habetler & D.M.Diwan; Acoustic Noise Reduction in sinusoidal PWM drives using a randomly modulated carrier, IEEE Trans on Power Electronics, vol. 6, No. 3, July 1991.
3. S.Y.R. Hui & S. Sathiakumar, Optimisation of microprocessor based random PWM scheme for power Inverters with low switching frequencies, IEEE 9th Applied Power Electronics Conference, Orlando, FL, pp 214-218, 1994.
4. Kjeld Thorborg, Power Electronics, Prentice Hall 1988.
5. Howard Demuth & Mark Beale, Neural Network Toolbox manual for use with MATLAB, Mathworks Inc; 1994.

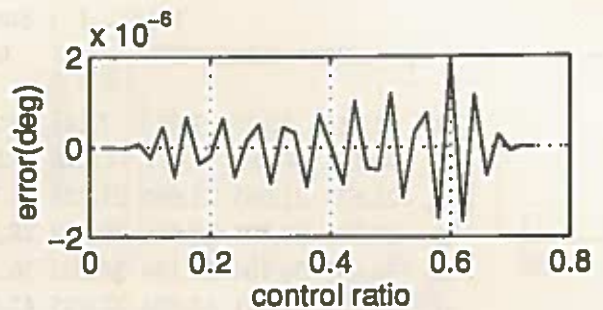


Fig. 3a, Training errors (α_{12})

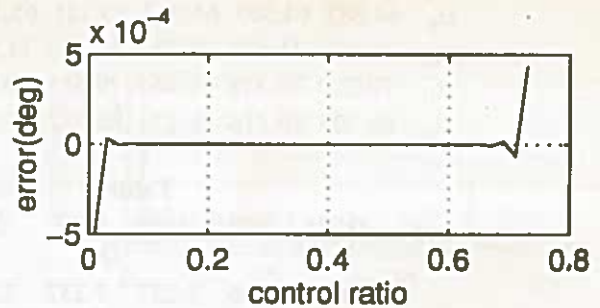


Fig. 3b, Interpolation errors (α_{12})

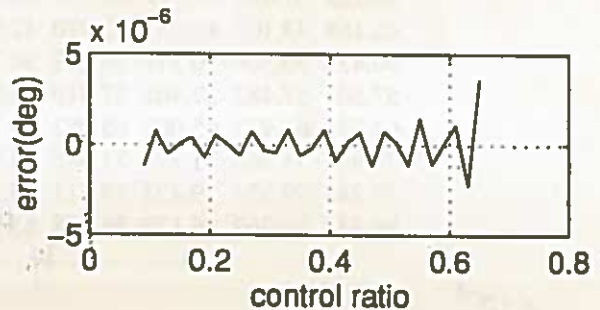


Fig. 3c, Interpolation errors (α_{12})

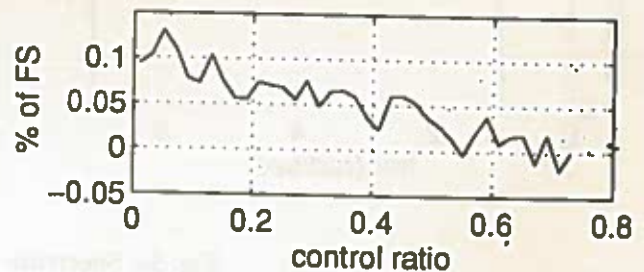


Fig. 4, Linearity error with NNet PWM

Table . 1 (Sample Training Data)

γ	0.02	0.04	0.06	0.08	0.10	0.12	0.14	0.16	0.18	0.20
α_1	7.211	7.222	7.232	7.242	7.252	7.261	7.269	7.278	7.285	7.292
α_2	14.376	14.352	14.327	14.302	14.275	14.248	14.220	14.192	14.162	14.132
α_3	21.633	21.665	21.695	21.725	21.754	21.781	21.807	21.831	21.855	21.877
α_4	28.755	28.708	28.661	28.612	28.561	28.509	28.456	28.401	28.345	28.287
α_5	36.053	36.104	36.154	36.202	36.249	36.293	36.336	36.378	36.417	36.455
α_6	43.136	43.071	43.004	42.935	42.865	42.793	42.719	42.643	42.566	42.487
α_7	50.469	50.537	50.604	50.669	50.732	50.793	50.853	50.910	50.966	51.020
α_8	57.521	57.442	57.360	57.278	57.193	57.107	57.020	56.930	56.839	56.746
α_9	64.882	64.963	65.043	65.121	65.198	65.274	65.348	65.421	65.493	65.562
α_{10}	71.912	71.823	71.733	71.643	71.551	71.458	71.364	71.268	71.172	71.074
α_{11}	79.289	79.378	79.467	79.555	79.642	79.729	79.815	79.901	79.986	80.070
α_{12}	86.308	86.216	86.124	86.032	85.939	85.846	85.753	85.659	85.565	85.471

Table . 2 (Sample Test Data)

γ	0.01	0.03	0.05	0.07	0.09	0.11	0.13	0.15	0.17	0.19
	7.205	7.216	7.227	7.237	7.247	7.256	7.265	7.273	7.281	7.289
	14.388	14.364	14.340	14.315	14.289	14.262	14.234	14.206	14.177	14.147
	21.616	21.649	21.680	21.710	21.739	21.767	21.794	21.819	21.843	21.866
	28.777	28.732	28.685	28.636	28.586	28.535	28.483	28.429	28.373	28.316
	36.026	36.076	36.129	36.178	36.226	36.271	36.315	36.357	36.398	36.436
	43.168	43.103	43.037	42.970	42.900	42.829	42.756	42.681	42.605	42.526
	50.435	50.504	50.571	50.637	50.700	50.763	50.823	50.882	50.938	50.993
	57.561	57.482	57.401	57.319	57.236	57.150	57.064	56.975	56.887	56.793
	64.841	64.922	65.003	65.082	65.160	65.236	65.311	65.385	65.457	65.528
	71.956	71.868	71.778	71.688	71.597	71.504	71.411	71.316	71.220	71.123
	79.244	79.334	79.423	79.511	79.599	79.686	79.772	79.858	79.943	80.028
	86.354	86.262	86.170	86.078	85.985	85.893	85.799	85.706	85.612	85.518

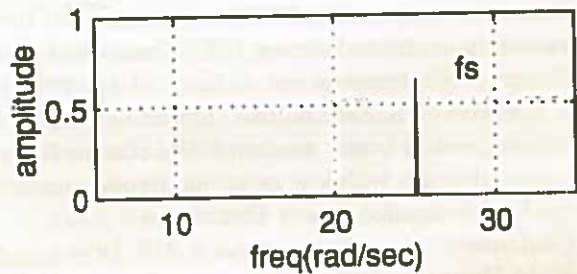
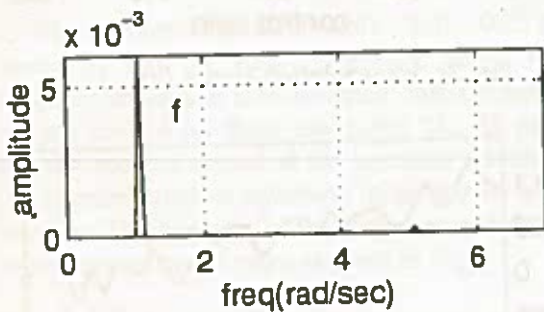


Fig. 5a, Spectrum of o/p ($\gamma = 0.01$)

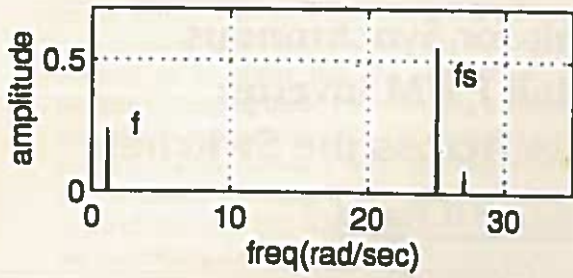


Fig. 5b, Spectrum of o/p ($\gamma = 0.37$)

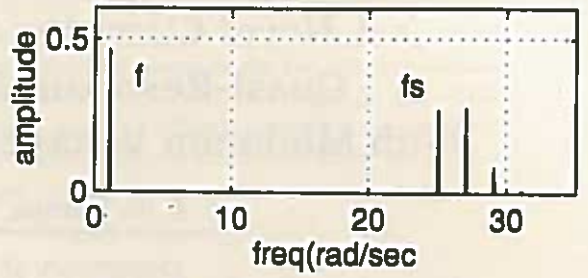


Fig. 5c, Spectrum of o/p ($\gamma = 0.73$)

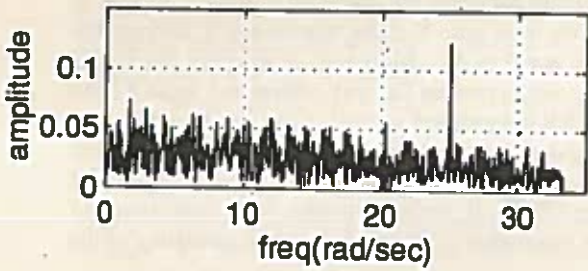


Fig 6 a , Spectrum ($\gamma = 0.01$) rand mod

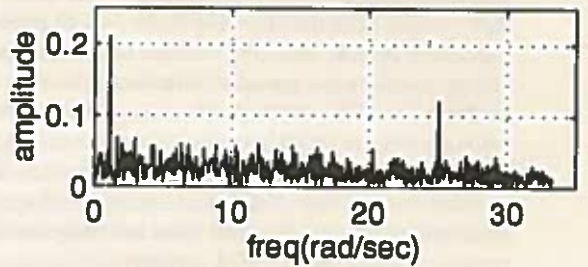


Fig 6 b , Spectrum ($\gamma = 0.37$) rand mod

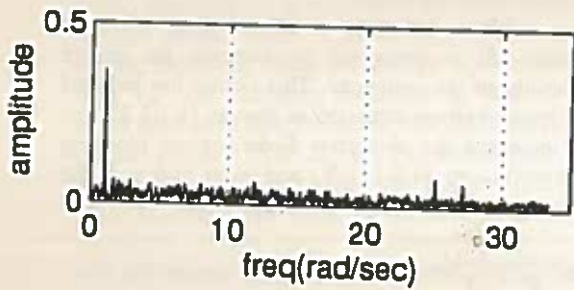


Fig 6 c , Spectrum ($\gamma = 0.73$) rand mod